# Investigation of quark-hadron phase-transition using an extended NJL model

Tong-Gyu Lee

(Kochi Univ. and JAEA)

Based on:

Prog. Theor. Exp. Phys. (2013) 013D02.

Collaborators:

Y. Tsue (Kochi Univ.),

J. da Providência, C. Providência (Univ. de Coimbra),

and M. Yamamura (Kansai Univ.).


— 513th ASRC Seminar/30th Hadron Group Seminar —

Apr. 26, 2013, JAEA-ASRC

# Introduction

(Non-perturbative aspects, phase diagram and low energy effective model of QCD)

# Introduction

- Basic building blocks of matter

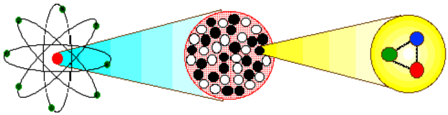

- Phenomenological aspects of QCD (Asymptotic freedom, Quark confinement)

Running coupling constant

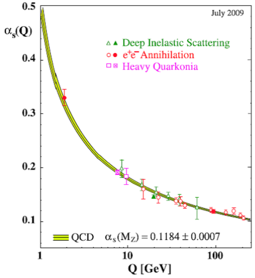


[ S. Bethke, Eur. Phys. J. C 64 (2009) ]

Anti-screening

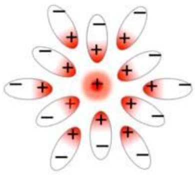

# Non-perturbative aspects of QCD

- Quantum chromodynamics (QCD)
  - ▷ A fundamental theory of strong interactions
    - ⇒ describes strongly interacting quark-hadron many-body systems
  - ▷ Low-energy regime
    - ⇒ quark and gluon interact non-perturbativelly
      (non-trivial vacuum structure: non-zero quark and gluon condensates)
    - ⇒ spontaneous chiral symmetry breaking, quark confinement, etc
  - ▷ At high-energy densities
    - ⇒ may occur a phase transition
      from a chiral symmetry breaking confined state (Hadron)
      to a chiral symmetric deconfined state (Quark-Gluon Plasma)
- QCD phase transition
  - ▷ Under extreme environments at high temperature and/or high density
    - ⇒ Early universe right after Big Bang : Hot QCD
      - → Quark-Gluon Plasma (quark-gluon many-body systems)
    - ⇒ Interior of compact objects such as neutron stars : Dense QCD
      - → Color superconductor (quark Cooper pair)
      - → Magnetar (quark ferromagnetism)

# QCD phase structure

▷ $H_2O$ phase diagram

- 3 states (ice, water, vapor)

- critical point, triple point

[ Schematic water phase diagram ]

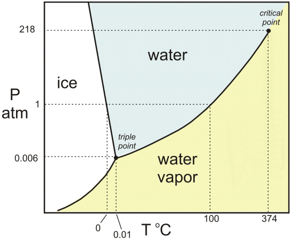


▷ QCD phase diagram

- 3 states ? (Hadron, QGP, CSC)

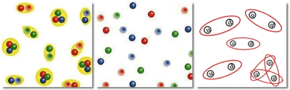

- How about phase transitions ?
- How about critical points ?

[ Schematic QCD phase diagram ]

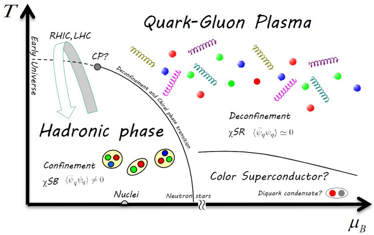

# QCD phase structure

▷ Cuprate high-$T_c$ SC phase diagram

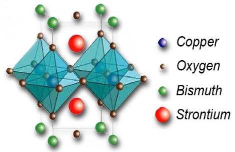


- Similar to QCD phase diagram ?
- Antiferromagnetism
  may relevant to QCD ?
- Quark-Hadron many-body systems

  ⇕ ?

  Strongly correlated electron systems

[ Schematic phase diagrams of QCD matters and of hole-doped cuprates ]

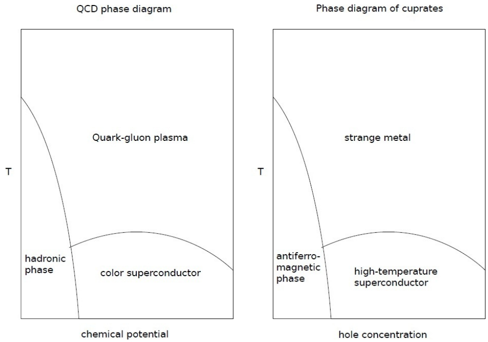

# Exploring the QCD phase structure

▷ Experimental exploration

- High-energy heavy-ion collision

  ⇒ creation of a hot QCD matter

  · Relativistic Heavy-ion Collider (RHIC)
  · Large Hadron Collider (LHC)

- High-intensity heavy-ion collision

  ⇒ creation of a dense QCD matter

  · Nuclotron-based Ion Collider fAcility (NICA)
  · Facility for Antiproton and Ion Research (FIAR)
  · Japan Proton Accelerator Research Complex (J-PARC)

▷ Theoretical exploration

- Perturbative QCD

  ⇒ perturbative calculations only work at asymptotically high temperatures and densities

- Lattice QCD

  ⇒ finite temperature regime → feasible
  ⇒ finite density regime → infeasible (Sign problem)

- Effective models

  ⇒ finite (moderate) density regime → rich structure

[ Schematic QCD phase diagram ]

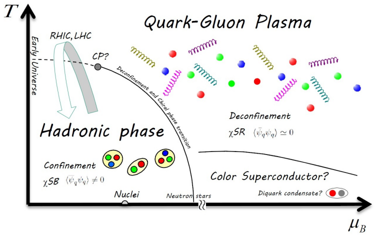

# Exploring the QCD phase structure

## ▷ Experimental exploration

- **High-energy heavy-ion collision**
  - ⇒ creation of a hot QCD matter
    - · Relativistic Heavy-ion Collider (RHIC)
    - · Large Hadron Collider (LHC)
- **High-intensity heavy-ion collision**
  - ⇒ creation of a dense QCD matter
    - · Nuclotron-based Ion Collider fAcility (NICA)
    - · Facility for Antiproton and Ion Research (FIAR)
    - · Japan Proton Accelerator Research Complex (J-PARC)

## ▷ Theoretical exploration

- **Perturbative QCD**
  - ⇒ perturbative calculations only work at asymptotically high temperatures and densities
- **Lattice QCD**
  - ⇒ finite temperature regime → feasible
  - ⇒ finite density regime → infeasible (Sign problem)
- **Effective models**
  - ⇒ finite (moderate) density regime → rich structure

[ Schematic QCD phase diagram ]

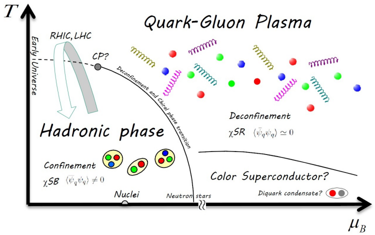


[ Recent QCD phase diagram (Fukushima et al, 2013) ]

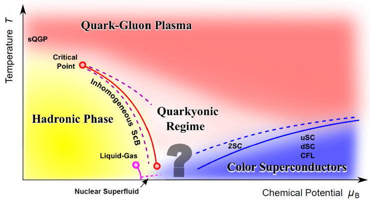

# Exploring the QCD phase structure

## ▷ Experimental exploration

- ▶ High-energy heavy-ion collision
  - ⇒ creation of a hot QCD matter
    - · Relativistic Heavy-ion Collider (RHIC)
    - · Large Hadron Collider (LHC)
- ▶ High-intensity heavy-ion collision
  - ⇒ creation of a dense QCD matter
    - · Nuclotron-based Ion Collider fAcility (NICA)
    - · Facility for Antiproton and Ion Research (FIAR)
    - · Japan Proton Accelerator Research Complex (J-PARC)

## ▷ Theoretical exploration

- ▶ Perturbative QCD
  - ⇒ perturbative calculations only work at asymptotically high temperatures and densities
- ▶ Lattice QCD
  - ⇒ finite temperature regime → feasible
  - ⇒ finite density regime → infeasible (Sign problem)
- ▶ Effective models
  - ⇒ finite (moderate) density regime → rich structure

[ Schematic QCD phase diagram ]

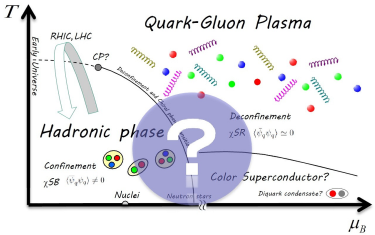


[ Recent QCD phase diagram (Fukushima et al, 2013) ]

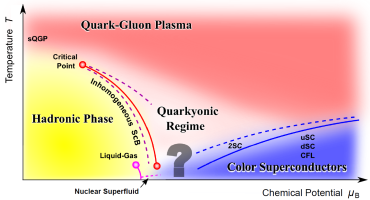

# Exploring the QCD phase structure

## ▷ Experimental exploration

- High-energy heavy-ion collision

  ⇒ creation of a hot QCD matter

  · Relativistic Heavy-ion Collider (RHIC)
  · Large Hadron Collider (LHC)

- High-intensity heavy-ion collision

  ⇒ creation of a dense QCD matter

  · Nuclotron-based Ion Collider fAcility (NICA)
  · Facility for Antiproton and Ion Research (FIAR)
  · Japan Proton Accelerator Research Complex (J-PARC)

## ▷ Theoretical exploration

- Perturbative QCD

  ⇒ perturbative calculations only work at asymptotically high temperatures and densities

- Lattice QCD

  ⇒ finite temperature regime → feasible

  ⇒ finite density regime → infeasible (Sign problem)

- Effective models

  ⇒ finite (moderate) density regime → rich structure

[ Schematic QCD phase diagram ]

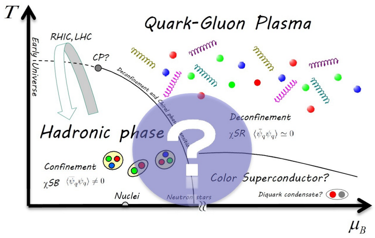


▷ we concentrate upon finite density systems

- chiral phase transition
- deconfinement phase transition (confinement problem)

⇓

- Quark-Hadron phase transition
- Effective model approach (NJL-type)

# Nambu-Jona-Lasinio (NJL) model

## ▷ Original NJL model

- Before the discovery of quarks, it was formulated as a model for nucleons (⇒ pion was described as a nucleon-antinucleon Goldstone excitation)
- Lagrangian density (2-flavor, massless) :

$$\mathcal{L}_{\rm NJL} = \overline{\psi}_N i\gamma^\mu \partial_\mu \psi_N + G_s^N \left[ (\overline{\psi}_N \psi_N)^2 + (\overline{\psi}_N i\gamma_5 \tau^a \psi_N)^2 \right]$$

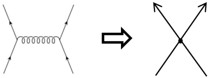

[Modelization of fermion-antifermion interaction : 4-point fermion interaction (Gs) ]

- Nucleon field $\psi_N$ is regarded as a fundamental field

## ▷ Quark NJL model

- After the establishment of QCD, it is reinterpreted as a model for quarks (⇒ vacuum is described by a quark-antiquark condensate $\langle \overline{\psi}_q \psi_q \rangle$)
- Under mean field approximation (MFA) :

$$\mathcal{L}_{\rm MF} = \overline{\psi}_q (i\gamma^\mu \partial_\mu - m_q)\psi_q - G_s^q \langle \overline{\psi}_q \psi_q \rangle^2$$

⇒ dynamical (constituent) quark mass : $m_q = -2G_s^q \langle \overline{\psi}_q \psi_q \rangle$ (gap equation)

# Extended NJL model for nuclear matter

## ▷ Nucleon NJL model

- A four-point interaction term (characteristic of NJL) 【H.Bohr et al, PRC71(2005)055203】 effectively comes out of a QCD-inspired many-body model for nucleons
  ( an effective string model ⇔ an NJL-type model (two-particle strings : chiral fields) )
- The bound nucleonic matter with spontaneously broken chiral symmetry is not possible within the original NJL model 【M.Buballa NP611(1996)393】
- Nuclear saturation properties (bulk static properties) is well produced by introducing an additional vector-vector 4-point and scalar-vector 8-point interaction
  【V.Koch et al, PLB185(1987)1; C.Providência et al, IJMPB17(2003)5209; S.A.Moszkowski et al, arXiv:nucl-th/0204047; T.J.Bürvenich et al, NPA729(2003)769; I.N.Mishustin et al, PR391(2004)363】
  ( an extended NJL model ⇔ Walecka-type model (nucleon : fundamental particle) )

## ▷ Extended NJL model with $G_{sv}^N$

- Lagrangian density (2-flavor, massless) :

$$\mathcal{L}_N = \bar{\psi}_N i\gamma^\mu \partial_\mu \psi_N + G_s^N \left[ (\bar{\psi}_N \psi_N)^2 + (\bar{\psi}_N i\gamma_5 \tau^a \psi_N)^2 \right] - G_v^N (\bar{\psi}_N \gamma^\mu \psi_N)^2 - G_{sv}^N \left[ (\bar{\psi}_N \psi_N)^2 + (\bar{\psi}_N i\gamma_5 \boldsymbol{\tau} \psi_N)^2 \right] (\bar{\psi}_N \gamma^\mu \psi_N)^2$$

- The term with $G_{sv}^N$ leads to an effective density-dependent coupling :

$$G_s^N \to G_s^N(\rho_N) = G_s^N(1 - G_{sv}^N / G_s^N \cdot \rho_N^2)$$

⇒ which makes an incompressibility lower 【S.A.Moszkowski et al, arXiv:nucl-th/0204047】

# Extended NJL model for quark matter

▷ Extended NJL model with $G^q_{sv}$

- Lagrangian density (2-flavor, massless) :

$$\mathcal{L}_q = \overline{\psi}_q i\gamma^\mu \partial_\mu \psi_q + G^q_s \left[ (\overline{\psi}_q \psi_q)^2 + (\overline{\psi}_q i\gamma_5 \tau^a \psi_q)^2 \right]$$
$$- G^q_v (\overline{\psi}_q \gamma^\mu \psi_q)^2 - G^q_{sv} \left[ (\overline{\psi}_q \psi_q)^2 + (\overline{\psi}_q i\gamma_5 \boldsymbol{\tau} \psi_q)^2 \right] (\overline{\psi}_q \gamma^\mu \psi_q)^2$$

- The term with $G^q_{sv}$ leads to an effective density-dependent coupling :

$$G^q_s \to G^q_s(\rho_q) = G^q_s(1 - G^q_{sv}/G^q_s \cdot \rho_q^2)$$

$\Rightarrow$ which pushes the chiral symmetry restoration point to the high-density side (which delays the chiral restoration 【S.A.Moszkowski et al, arXiv:nucl-th/0204047】 )

- $G^q_{sv}$ : free parameter

$\Rightarrow$ a tuning parameter of the chiral restoration point 【Y.Tsue et al, PTP123(2010)138】

# Motivation

## ▷ Objective

- To investigate the quark-hadron phase transition at finite temperature and density
- To draw the phase diagram on the temperature-baryon chemical potential plane

– This talk –

- Hadronic phase side ⇒ isospin-symmetric nuclear matter ($m_N = (m_n + m_p)/2$)
- Quark phase side ⇒ free quark phase (non-superconducting quark matter)

## ▷ Treatment

- Extended NJL model for nuclear and quark matters (2-flavor)

  including scalar-vector eight-point interaction

  ⇒ Nuclear matter : Reproduction of a rather reasonable nuclear saturation properties

  ⇒ Quark matter : Influence on the chiral phase transition (turning of chiral restoration)
- Pressure comparison

  ⇒ Determination of physically realized phase which has the largest pressure

  ⇒ Description of the quark-hadron phase transition

# Outline

# Formalism

(Extended NJL model + Mean field approximation, Thermodynamics)

# Extended NJL Lagrangian for nuclear and quark matters

- Lagrangian density for nuclear and quark matters :

$$\mathcal{L}_i = \bar{\psi}_i i\gamma^\mu \partial_\mu \psi_i + G_s^i \left[ (\bar{\psi}_i \psi_i)^2 + (\bar{\psi}_i i\gamma_5 \boldsymbol{\tau} \psi_i)^2 \right] - G_v^i (\bar{\psi}_i \gamma^\mu \psi_i)^2 - G_{sv}^i \left[ (\bar{\psi}_i \psi_i)^2 + (\bar{\psi}_i i\gamma_5 \boldsymbol{\tau} \psi_i)^2 \right] (\bar{\psi}_i \gamma^\mu \psi_i)^2$$

First two terms : the original NJL Lagrangian (scalar-type 4-point interaction)
Third term : the vector-vector repulsive term (vector-type 4-point interaction)
Last term : the scalar-vector coupling term (scalar-vector-type 8-point interaction)

- For nuclear matter $(i = N)$
  - $\Rightarrow$ $\psi_N$ : nucleon field (fundamental, not composite)
  - $\Rightarrow$ $N_f^N = 2,\ N_c^N = 1,\ G_v^N \neq 0,\ G_{sv}^N \neq 0,\ \Lambda_N$
- For quark matter $(i = q)$
  - $\Rightarrow$ $\psi_q$ : quark field
  - $\Rightarrow$ $N_f^q = 2,\ N_c^q = 3,\ G_v^q = 0,\ G_{sv}^q \neq 0,\ \Lambda_q$ (the effects of $G_v^q$ is well-known) 【M.Kitazawa et al, PTP108(2002)929】

# Mean field approximation

- Mean field approximation :

$$\mathcal{L}_i^{MF} = \overline{\psi}_i(i\gamma^\mu\partial_\mu - \underline{m_i})\psi_i + \widetilde{\mu}_i\overline{\psi}_i\gamma^0\psi_i + C_i$$

$m_i$ : Effective mass

$$\mathcal{H}_i^{MF} = -i\overline{\psi}_i\boldsymbol{\gamma}\cdot\nabla\psi_i + m_i\overline{\psi}_i\psi_i + \widetilde{\mu}_i\overline{\psi}_i\gamma^0\psi_i - C_i$$

with

$$C_i \equiv -G_s^i\langle\langle\overline{\psi}_i\psi_i\rangle\rangle^2 + G_v^i\langle\langle\overline{\psi}_i\gamma^0\psi_i\rangle\rangle^2 + 3G_{sv}^i\langle\langle\overline{\psi}_i\psi_i\rangle\rangle^2\langle\langle\overline{\psi}_i\gamma^0\psi_i\rangle\rangle^2$$

$$\underline{m_i = -2\left[G_s^i + 2G_{sv}^i\langle\langle\overline{\psi}_i\gamma^0\psi_i\rangle\rangle^2\right]\langle\langle\overline{\psi}_i\psi_i\rangle\rangle}$$

: Gap equation

$$\widetilde{\mu}_i = 2\left[G_v^i + 2G_{sv}^i\langle\langle\overline{\psi}_i\psi_i\rangle\rangle^2\right]\langle\langle\overline{\psi}_i\gamma^0\psi_i\rangle\rangle$$

bilinear quantities — expectation values — fluctuations

MFA : $\overline{\psi}_i\Gamma\psi_i \rightarrow \langle\langle\overline{\psi}_i\Gamma\psi_i\rangle\rangle + (\overline{\psi}_i\Gamma\psi_i - \langle\langle\overline{\psi}_i\Gamma\psi_i\rangle\rangle)$ $\quad \Gamma = 1, \gamma_5, \gamma^\mu$, etc.

$\Rightarrow$ four-point interactions : $(\overline{\psi}_i\Gamma\psi_i)^2 \sim -\langle\langle\overline{\psi}_i\Gamma\psi_i\rangle\rangle^2 + 2\overline{\psi}_i\Gamma\psi_i\langle\langle\overline{\psi}_i\Gamma\psi_i\rangle\rangle$

fermionic condensate — fermion number density

$\langle\langle\overline{\psi}_i\psi_i\rangle\rangle \neq 0, \quad \rho_i \equiv \langle\langle\psi_i^\dagger\psi_i\rangle\rangle = \langle\langle\overline{\psi}_i\gamma^0\psi_i\rangle\rangle \neq 0,$ others $= 0$

# Finite density and temperature systems

## Finite density system

- Introduce the chemical potential $\mu_i$ :

$$\begin{aligned}\mathcal{H}'_i &= \mathcal{H}_i^{MF} - \underline{\mu_i}\psi_i^\dagger\psi_i \\ &= -i\overline{\psi}_i\boldsymbol{\gamma}\cdot\nabla\psi_i + m_i\overline{\psi}_i\psi_i - \mu_i^r\overline{\psi}_i\gamma^0\psi_i - C_i\end{aligned}$$

⇒ The effective chemical potential $\mu_i^r$ :

$$\begin{aligned}\mu_i^r &= \mu_i - \widetilde{\mu}_i \\ &= \mu_i - 2\left[G_v^i + G_{sv}^i\langle\langle\overline{\psi}_i\psi_i\rangle\rangle^2\right]\langle\langle\overline{\psi}_i\gamma^0\psi_i\rangle\rangle\end{aligned}$$

## Finite temperature system

- Matsubara formalism :

$$\int\frac{d^4\boldsymbol{p}}{i(2\pi)^4}\,f(p_0,\boldsymbol{p}) \longrightarrow T\sum_{n=-\infty}^{\infty}\int\frac{d^3\boldsymbol{p}}{(2\pi)^3}\,f(i\omega_n+\mu_i,\boldsymbol{p})$$

Matsubara frequency : $\omega_n = (2n+1)\pi T$ (n: integer, $T(=1/\beta)$: temperature)

⇒ $\langle\langle\overline{\psi}_i\psi_i\rangle\rangle_{(T>0)}$ : Finite-temperature expectation value or thermal average

# Self-consistent equation for $m_i$

- NJL gap equation with $G_{sv}^i$ :

$$m_i = \underbrace{-2G_s^i\left[1-\frac{G_{sv}^i}{G_s^i}\langle\langle\overline{\psi}_i\gamma^0\psi_i\rangle\rangle^2\right]}_{\text{Density-dependent scalar coupling : } G_s^i(\rho_i)}\langle\langle\overline{\psi}_i\psi_i\rangle\rangle$$

where

$$\langle\langle\overline{\psi}_i\psi_i\rangle\rangle = \nu_i\int\frac{d^3\boldsymbol{p}}{(2\pi)^3}\frac{m_i}{\sqrt{\boldsymbol{p}^2+m_i^2}}(n_+^i-n_-^i)$$

$$\langle\langle\overline{\psi}_i\gamma^0\psi_i\rangle\rangle\ (=\rho_i) = \nu_i\int\frac{d^3\boldsymbol{p}}{(2\pi)^3}(n_+^i+n_-^i-1)$$

with

$$\nu_i = 2N_f^iN_c^i, \quad n_\pm^i = \left[e^{\beta(\pm\sqrt{\boldsymbol{p}^2+m_i^2}-\mu_i^r)}+1\right]^{-1}$$

Degenerate factor — Fermion number distribution function

$$\beta = 1/T, \quad \mu_i^r = \mu_i - 2\left[G_v^i + G_{sv}^i\langle\langle\overline{\psi}_i\psi_i\rangle\rangle^2\right]\rho_i$$

Temperature — Effective chemical potential

# Stable solution in gap-solutions

▷ Thermodynamic potential

- The gap equation might have more than one solution, so that a criterion is required to decide which solution is the correct one.
- Knowledge of statistical physics: Equilibrium state (for fixed $T$, $\mu_i^r$) is given by minimizing the thermodynamic potential density $\omega_i$. (It is appropriate to use the thermodynamic potential since $T$, $\mu_i^r$ are fixed and $\rho_i$ can vary.)
- The stable gap-solution is the solution which corresponds to the global minimum of $\omega_i$.

▷ Pressure

- From thermodynamic relations, thermodynamic quantities can be derived by $\omega_q$: Pressure is given by $p_q(T, \mu_q) = -\omega_q(T, \mu_q)$.
- The stable gap-solution also corresponds to the solution which leads to the largest pressure.

$\Rightarrow$ Here, we calculate the pressure in order to determine the stable gap-solution.

# Pressure

- Pressure of nuclear and quark matters :

$$p_i(T,\mu_i) \;=\; -\left[\langle\langle\mathcal{H}_i^{MF}\rangle\rangle_{(T,\mu_i)} - \langle\langle\mathcal{H}_i^{MF}\rangle\rangle_{(T=0,\ \mu_i=m_i(T=0))}\right] + \mu_i\langle\langle\mathcal{N}_i\rangle\rangle + T\langle\langle S_i\rangle\rangle$$

( Normalization: $p_i(0, m_{i\,(T=0)}) = 0$ where $\mu_i = m_{i\,(T=0)}$ leads to $\rho_i = 0$ )

where

$$\begin{aligned}
\langle\langle\mathcal{H}_i^{MF}\rangle\rangle &= \langle\langle\overline{\psi}_i(\boldsymbol{\gamma}\cdot\boldsymbol{p})\psi_i\rangle\rangle - G_s^i\langle\langle\overline{\psi}_i\psi_i\rangle\rangle^2 \\
&\qquad + G_v^i\langle\langle\overline{\psi}_i\gamma^0\psi_i\rangle\rangle^2 + G_{sv}^i\langle\langle\overline{\psi}_i\psi_i\rangle\rangle^2\langle\langle\overline{\psi}_i\gamma^0\psi_i\rangle\rangle^2 \\
\langle\langle\mathcal{N}_i\rangle\rangle &= \langle\langle\overline{\psi}_i\gamma^0\psi_i\rangle\rangle = \rho_i \\
\langle\langle S_i\rangle\rangle &= -\nu_i\int\frac{d^3\boldsymbol{p}}{(2\pi)^3}\left[\, n_+^i\ln n_+^i + (1-n_+^i)\ln(1-n_+^i)\right. \\
&\qquad \left. + n_-^i\ln n_-^i + (1-n_-^i)\ln(1-n_-^i)\,\right]
\end{aligned}$$

and

$$\langle\langle\overline{\psi}_i(\boldsymbol{\gamma}\cdot\boldsymbol{p})\psi_i\rangle\rangle = \nu_i\int\frac{d^3\boldsymbol{p}}{(2\pi)^3}\frac{\boldsymbol{p}^2}{\sqrt{\boldsymbol{p}^2+m_i^2}}(n_+^i - n_-^i)$$

# Numerical Results

Parameter sets for nuclear and quark matters

# Parameter set

- Nuclear matter
  - Model parameters : $G_s^N$, $G_v^N$, $G_{sv}^N$, $\Lambda_N$ 3-momentum cutoff
  - Conditions :

$m_N(\rho_N = 0) = 939$ MeV, $\rho_N^0 = 0.17$ fm$^{-3}$ Normal nuclear density

$m_N(\rho_N = \rho_N^0) = 0.6 m_N(\rho_N = 0)$ MeV Ratio of in-medium to vacuum nucleon mass: 0.6

$W_N(\rho_N = \rho_N^0) = -15$ MeV Binding energy per single nucleon:

$$W_N(\rho_N) = \frac{\langle\langle \mathcal{H}_i^{MF} \rangle\rangle(T=0,\ \rho_N) - \langle\langle \mathcal{H}_i^{MF} \rangle\rangle(T=0,\ \rho_N=0)}{\rho_N} - m_N(\rho_N=0)$$

---

- Energy density per single nucleon $W_N$ vs Normal nuclear density $\rho_N/\rho_N^0$

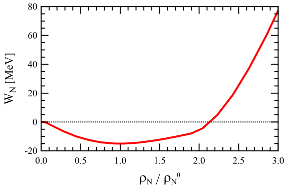


- Incompressibility of nuclear matter

$$K = 9\rho_N^0 \frac{\partial^2 W_N(\rho_N)}{\partial \rho_N^2}\Bigg|_{\rho_N = \rho_N^0}$$

$\simeq 260$ MeV

$\Rightarrow$ The nuclear matter saturation property is well reproduced.

# Parameter set

- Quark matter
  - Model parameters : $G_s^q, G_{sv}^q, \Lambda_q$
  - Conditions :

    $m_q(\rho_q{=}0) = 313$ MeV  vacuum quark mass

    $f_\pi = 93$ MeV  pion decay constant
  - Free parameter : $G_{sv}^q$
  - $m_q(\rho_q/3 = \rho_N^0) = 0.6 m_q(\rho_q{=}0)$ MeV $\leftarrow G_{sv}^q = 0$

    $m_q(\rho_q/3 = \rho_N^0) = 0.625 m_q(\rho_q{=}0)$ MeV $\rightarrow G_{sv}^q \Lambda_q^8 = -68.4$

    $m_q(\rho_q/3 = \rho_N^0) = 0.63 m_q(\rho_q{=}0)$ MeV $\rightarrow G_{sv}^q \Lambda_q^8 = -81.9$

---

- $m_q = -2G_s^q \langle\langle \overline{\psi}_q \psi_q \rangle\rangle_{(T=0)} = \frac{2}{\pi^2} G_s^q N_f N_c m_q \int_0^{\Lambda_q} d|\boldsymbol{p}| \frac{\boldsymbol{p}^2}{\sqrt{\boldsymbol{p}^2 + m_q^2}} = 313$ MeV
- $f_\pi^2 = \frac{1}{2\pi^2} N_c m_q^2 \int_0^{\Lambda_q} d|\boldsymbol{p}| \frac{\boldsymbol{p}^2}{(\boldsymbol{p}^2 + m_q^2)^{3/2}} = (93 \text{ MeV})^2$
- In the case of $G_{sv}^q = 0$,

$$m_q(\rho_q^0/3 = \rho_N^0) \approx 187 \text{ MeV} \sim 0.6 m_q(\rho_N^0 = 0)$$

# Parameter set

- The parameter sets for nuclear $(i = N)$ and quark matters $(i = q)$

【Y. Tsue, J. da Providência, C Providência and M. Yamamura, Prog. Theor. Phys. 123, (2010), 1013】

| | | | |
|---|---|---|---|
| $\Lambda_N$ | 377.8 MeV | $\Lambda_q$ | 653.961 MeV |
| $G_s^N \Lambda_N^2$ | 19.2596 | $G_s^q \Lambda_q^2$ | 2.13922 |
| $G_v^N \Lambda_N^2$ | $-1069.89$ | $G_v^q \Lambda_q^2$ | 0 |
| $G_{sv}^N \Lambda_N^8$ | 17.9824 | $G_{sv}^q \Lambda_q^8$ | free*) |

*) $G_{sv}^q = 0, \; G_{sv}^q \Lambda_q^8 = -68.4, \; G_{sv}^q \Lambda_q^8 = -81.9$ 【T.-G. Lee et al, PETP(2013)013D02.】

# Numerical Results

with $G^q_{sv}\Lambda^8_q = -68.4$

# Numerical Results with $G^q_{sv}\Lambda^8_q = -68.4$

▶ Dynamical quark mass $m_q$
vs Quark chemical potential $\mu_q$

▷ Quark number density $\rho_q$
vs Quark chemical potential $\mu_q$

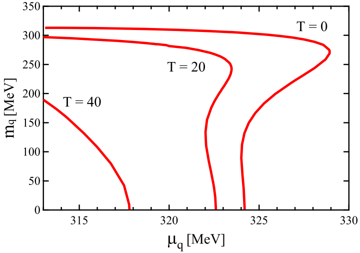


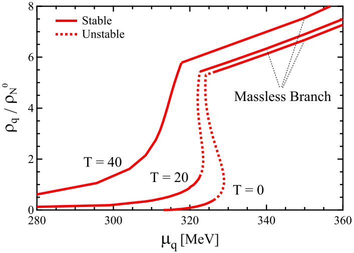


---

▷ Unphysical regions which have unstable solutions

Comparison of pressure

⟹ Determine the physically realized solution (stable solution)

---

▷ The solution with largest pressure = The physically realized solution

# Numerical Results with $G_{sv}^q \Lambda_q^8 = -68.4$

▶ Pressure of quark matter $p_q$ vs Quark chemical potential $\mu_q$

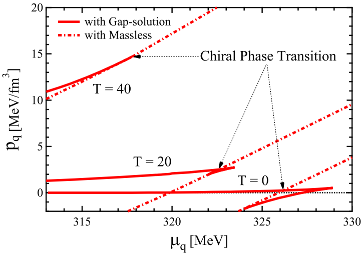


▷ Quark number density $\rho_q$ vs Quark chemical potential $\mu_q$

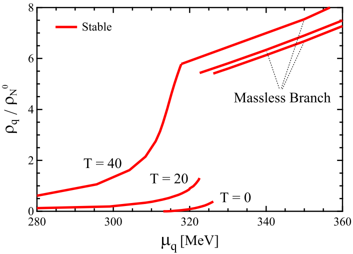


---

▷ $T = 0$ MeV

- $\mu_q^{\text{chiral}} \approx 326$ MeV : Chiral phase transition
- $\rho_q^{\text{coex}} = 0.38\rho_N^0 \sim 5.41\rho_N^0$ : 1st-order phase transition

  $(\rho_B = 0.13\rho_N^0 \sim 1.80\rho_N^0)$

---

# Numerical Results with $G_{sv}^q \Lambda_q^8 = -68.4$

- ▶ Pressure of quark matter $p_q$ vs Quark chemical potential $\mu_q$
- ▷ Quark number density $\rho_q$ vs Quark chemical potential $\mu_q$

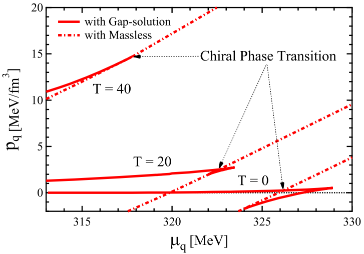


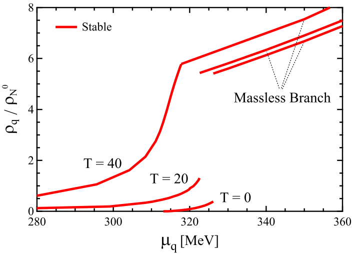


▷ $T = 20$ MeV

- $\mu_q^{\text{chiral}} \approx 323$ MeV : Chiral phase transition
- $\rho_q^{\text{coex}} = 1.30\rho_N^0 \sim 5.41\rho_N^0$ : 1st-order phase transition

  $(\rho_B = 0.43\rho_N^0 \sim 1.80\rho_N^0)$

# Numerical Results with $G^q_{sv}\Lambda^8_q = -68.4$

▶ Pressure of quark matter $p_q$ vs Quark chemical potential $\mu_q$

▷ Quark number density $\rho_q$ vs Quark chemical potential $\mu_q$

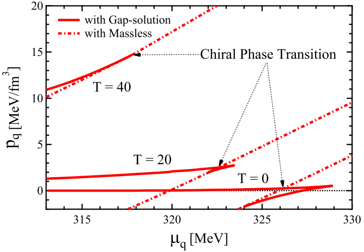


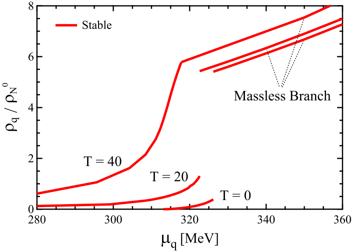


▷ $T = 40$ MeV

- $\mu_q^{\text{chiral}} \approx 318$ MeV : Chiral phase transition
- $\rho_q^{\text{chiral}} \sim 5.78\rho_N^0$ : 2nd-order phase transition
  $(\rho_B \sim 1.93\rho_N^0)$

# Quark-Hadron phase transition

with $G^q_{sv}\Lambda^8_q = -68.4$

# Numerical Results with $G_{sv}^q \Lambda_q^8 = -68.4$

▶ Pressure $p_i$

vs Baryon number density $\mu_B$

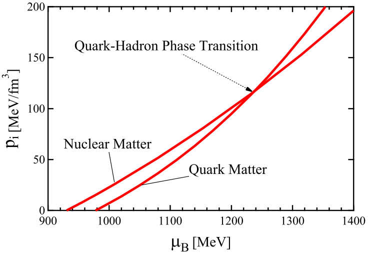


▷ Pressure $p_i/p_0$

vs Baryon number density $\mu_B/\rho_N^0$

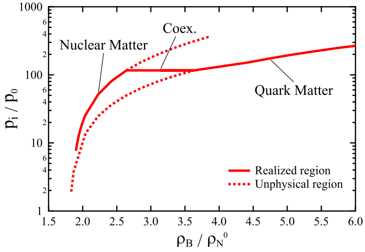


▷ The condition for thermodynamic equilibrium

between the hadron and quark phases*) :

$$p_N(T, \mu_N) = p_q(T, 3\mu_q)$$

*) The condition for chemical equilibrium : $\mu_N(T) = 3\mu_q(T)$ $(= \mu_B(T))$

# Numerical Results with $G_{sv}^q \Lambda_q^8 = -68.4$

▶ Pressure $p_i$
vs Baryon number density $\mu_B$

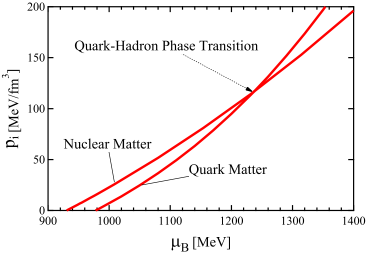


▷ Pressure $p_i/p_0$
vs Baryon number density $\mu_B/\rho_N^0$

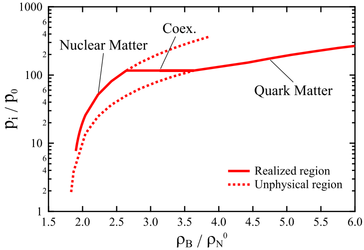


▷ $T = 0$ MeV

- $\mu_B^{\text{QH}} \approx 1236$ MeV : Quark-Hadron phase transition
- $\rho_B^{\text{coex}} = 2.64\rho_N^0 \sim 3.63\rho_N^0$ : 1st-order phase transition
  $(\rho_N = 2.64\rho_N^0 \sim \rho_q = 10.9\rho_N^0)$

# Numerical Results with $G_{sv}^{q}\Lambda_q^8 = -68.4$

- Pressure $p_i$

  vs Baryon number density $\mu_B$

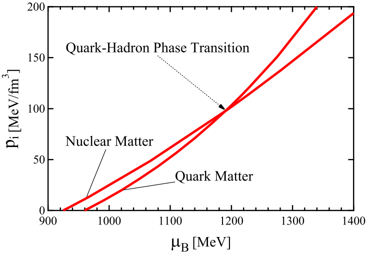


- Pressure $p_i/p_0$

  vs Baryon number density $\mu_B/\rho_N^0$

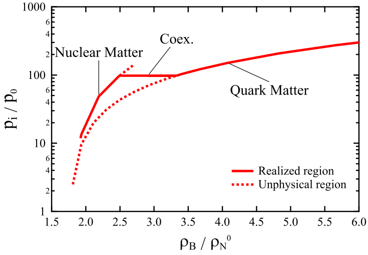


---

▷ $T = 20$ MeV

- $\mu_B^{\text{QH}} \approx 1190$ MeV : Quark-Hadron phase transition
- $\rho_B^{\text{coex}} = 2.49\rho_N^0 \sim 9.99\rho_N^0$ : 1st-order phase transition

  $(\rho_N = 2.49\rho_N^0 \sim \rho_q = 3.33\rho_N^0)$

---

# Numerical Results with $G^q_{sv}\Lambda^8_q = -68.4$

- ▶ Pressure $p_i$
  vs Baryon number density $\mu_B$

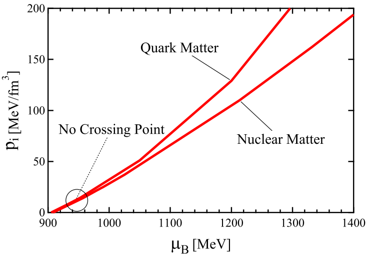


- ▷ Pressure $p_i/p_0$
  vs Baryon number density $\mu_B/\rho^0_N$

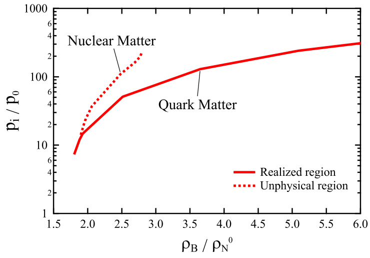


---

▷ $T = 40$ MeV

- There is no crossing point.
  ⇒ 1st-order quark-hadron phase transition disappears.

---

# Phase diagram $(\mu_B, T)$

- Phase diagram with $G^q_{sv}\Lambda^8_q = -68.4$

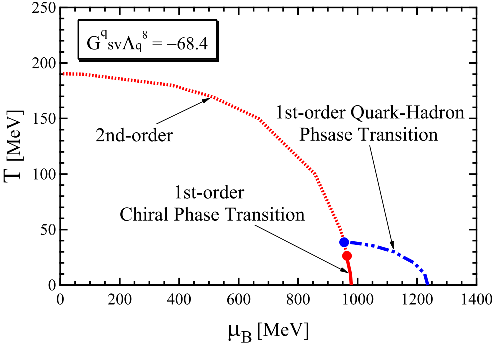


▷ Low-$T$ : 1st-order chiral phase transition, 1st-order quark-hadron phase transition
▷ High-$T$ : 2nd-order chiral phase transition
▷ Moderate-$\mu_B$ : Chiral restoration + Nuclear phase ( ⇒ Quarkyonic-like phase ? )

# $G_{sv}^{q}$-dependence of phase diagram

# $G^q_{sv}$-dependence of phase diagram

- Phase diagram with no scalar-vector interaction

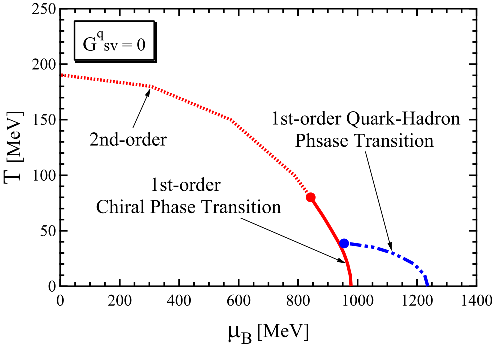


| | phase transition | | critical end point | | emerges | | terminates | |
|---|---|---|---|---|---|---|---|---|
| ▷ | $1^{st}$-order chiral phase transition | : | $(\mu_B, T)$ | $\simeq$ | $(978, 0)$ | $\rightarrow$ | $(842, 80)$ | MeV |
| ▷ | $2^{nd}$-order chiral phase transition | : | $(\mu_B, T)$ | $\simeq$ | $(842, 80)$ | $\rightarrow$ | $(0, 190)$ | MeV |
| ▷ | $1^{st}$-order quark-hadron transition | : | $(\mu_B, T)$ | $\simeq$ | $(1236, 0)$ | $\rightarrow$ | $(955, 39)$ | MeV |

# $G^q_{sv}$-dependence of phase diagram

- Phase diagram with scalar-vector interaction

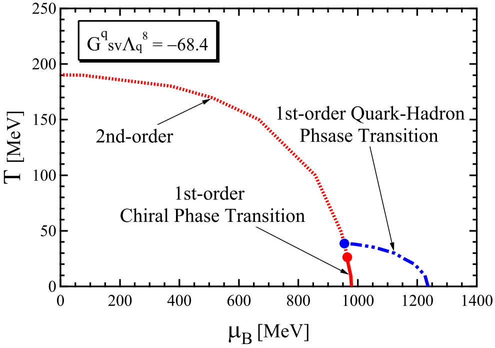


| | phase transition | | critical end point | | emerges | | terminates | |
|---|---|---|---|---|---|---|---|---|
| ▷ | 1st-order chiral phase transition | : | $(\mu_B, T)$ | $\simeq$ | $(979, 0)$ | $\to$ | $(964, 26)$ | MeV |
| ▷ | 2nd-order chiral phase transition | : | $(\mu_B, T)$ | $\simeq$ | $(964, 26)$ | $\to$ | $(0, 190)$ | MeV |
| ▷ | 1st-order quark-hadron transition | : | $(\mu_B, T)$ | $\simeq$ | $(1236, 0)$ | $\to$ | $(955, 39)$ | MeV |

# $G^q_{sv}$-dependence of phase diagram

- Phase diagram with stronger scalar-vector interaction

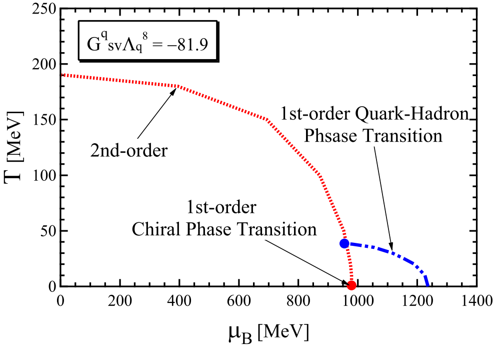


| | phase transition | | critical end point | | emerges | | terminates |
|---|---|---|---|---|---|---|---|
| ▷ | 1st-order chiral phase transition | : | $(\mu_B, T)$ | $\simeq$ | $(979, 0)$ | $\rightarrow$ | $(979, 1)$ MeV |
| ▷ | 2nd-order chiral phase transition | : | $(\mu_B, T)$ | $\simeq$ | $(979, 1)$ | $\rightarrow$ | $(0, 190)$ MeV |
| ▷ | 1st-order quark-hadron transition | : | $(\mu_B, T)$ | $\simeq$ | $(1236, 0)$ | $\rightarrow$ | $(955, 39)$ MeV |

# $G_{sv}^{q}$-independence of phase boundary

▷ $G_{sv}^{q}$-independence of the quark-hadron phase transition

- There is no influence on the 1st-order quark-hadron phase transition.
  - Quark-hadron phase transition occurs after chiral restoration.

    $\Rightarrow \ m_q = 0, \ \langle\langle \overline{\psi}_q \psi_q \rangle\rangle = 0$
  - $G_{sv}^{q}$-independence of pressure $p_q$

$$p_q(T,\ \mu_q) = -\left[\langle\langle \mathcal{H}_q^{MF} \rangle\rangle_{(T,\mu_q)} - \langle\langle \mathcal{H}_q^{MF} \rangle\rangle_{(T=0,\ \rho_q=0)}\right] + \mu_q \langle\langle \mathcal{N}_q \rangle\rangle + T\langle\langle S_q \rangle\rangle$$

$$\langle\langle \mathcal{H}_q^{MF} \rangle\rangle = \langle\langle \overline{\psi}_q (\boldsymbol{\gamma}\cdot\boldsymbol{p})\psi_q \rangle\rangle - G_s^q \langle\langle \overline{\psi}_q \psi_q \rangle\rangle^2 + G_v^q \langle\langle \overline{\psi}_q \gamma^0 \psi_q \rangle\rangle^2 + G_{sv}^q \langle\langle \overline{\psi}_q \psi_q \rangle\rangle^2 \langle\langle \overline{\psi}_q \gamma^0 \psi_q \rangle\rangle^2$$

$$\mu_q^r = \mu_q - 2\left[G_v^q + G_{sv}^q \langle\langle \overline{\psi}_q \psi_q \rangle\rangle^2\right] \langle\langle \overline{\psi}_q \gamma^0 \psi_q \rangle\rangle$$

$\Rightarrow$ $\langle\langle \mathcal{H}_i^{MF} \rangle\rangle$ and $\mu_q^r$ do not depend on $G_{sv}^q$ due to $\langle\langle \overline{\psi}_q \psi_i \rangle\rangle = 0$.

# Summary

— Concluding Remarks —

# Summary

▷ We presented the treatment of the quark-hadron phase transition by using the extended NJL model for nuclear and quark matters with scalar-vector eight-point interaction.

- Numerical results
  - $1^{st}$-order quark-hadron phase transition is described.
  - $1^{st}$ and $2^{nd}$-order chiral phase transition is described.
  - An exotic phase, i.e., the nuclear phase, while the chiral symmetry is restored in terms of the quark matter, appears just before deconfinment.

    ⇒ Quarkyonic-like phase 【L.McLerran et al, NPA796(2007)83】

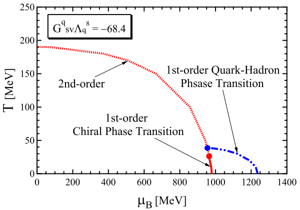

# Summary

▷ We presented the treatment of the quark-hadron phase transition by using the extended NJL model for nuclear and quark matters with scalar-vector eight-point interaction.

- $G^q_{sv}$-dependence on the phase diagram
  - Does not affect to the 1st-order quark-hadron phase transition.
    ⇒ The phase boundary is not changed. ($G^q_{sv}$-independence)
  - Affects the chiral phase transition. ($G^q_{sv}$-dependence)
    ⇒ Critical line of 1st-order shrinks with increasing $G^q_{sv}$.
    ⇒ Moves critical end point toward a larger $\mu_B$ and a lower $T$.

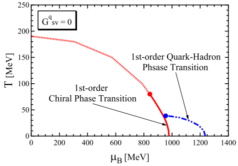


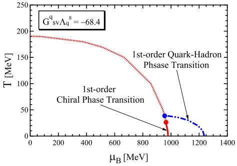


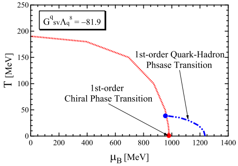

# Summary

## Future work

- Consideration of the color-superconducting phase

  $\Rightarrow$ Pairing interaction (CSC in quark phase, Nuclear superfluidity in nuclear phase)

- e.g. Quark-pair interaction $\mathcal{L}^q_c$ : (2SC)【Kitazawa et al, PTP108(2002)929】

$$\mathcal{L}^q_c = G^q_c \sum_{\alpha=2,5,7} \left[ (\overline{\psi}_q i\gamma_5 \tau_2 \lambda_\alpha \psi^C_q)(\overline{\psi}^C_q i\gamma_5 \tau_2 \lambda_\alpha \psi_q) + (\overline{\psi}_q \tau_2 \lambda_\alpha \psi^C_q)(\overline{\psi}^C_q \tau_2 \lambda_\alpha \psi_q) \right]$$

where $\psi^C_q = C\overline{\psi}^T_q$ and $\overline{\psi}^C_q = \psi^T_q C$ with $C = i\gamma^2\gamma^0$

- Assumption of the neutron star matter

  $\Rightarrow$ Phase transition between neutron matter and quark matter

  ($\rightarrow$ Physics of neutron stars)

- e.g. Pure neutron matter ($\nu_N = 4 \Rightarrow 2,\ p + e^- \rightarrow n + \mu_e$)

# Thank you for your attention!

# Back up

# Expectation values

**Expectation values** ( T = 0 )

$$\langle\overline{\psi}_i\psi_i\rangle = -\int\frac{d^4p}{i(2\pi)^4}\mathrm{Tr}(iS_i(p)) = -4N_c^iN_f^im_i\int\frac{d^4p}{i(2\pi)^4}\frac{1}{p^2-m_i^2-i\epsilon}$$

$$\langle\overline{\psi}_i\gamma^0\psi_i\rangle = -\int\frac{d^4p}{i(2\pi)^4}\mathrm{Tr}(\gamma^0 iS_i(p)) = -4N_c^iN_f^i\int\frac{d^4p}{i(2\pi)^4}\frac{p^0}{p^2-m_i^2-i\epsilon}$$

$$\langle\overline{\psi}_i(\boldsymbol{\gamma}\cdot\mathbf{p})\psi_i\rangle = -\int\frac{d^4p}{i(2\pi)^4}\mathrm{Tr}(\boldsymbol{\gamma}\cdot\mathbf{p}iS_i(p)) = -4N_c^iN_f^im_i\int\frac{d^4p}{i(2\pi)^4}\frac{p^2}{p^2-m_i^2-i\epsilon}$$

- $iS_i(p) = 1/(p^\mu\gamma_\mu - m_i - i\epsilon)$ ; fermion propagator
- $N_f^i$ ; flavor number ( $N_f^N = 2,\ N_f^q = 2$ )
- $N_c^i$ ; color number ( $N_c^N = 1,\ N_c^q = 3$ )

↓

- Matsubara sum $\int dp_0/(2\pi) \to iT\sum_{n=-\infty}^{\infty}$
- Matsubara's frequency $p_4 \to \omega_n = (2n+1)\pi T$ ( $T = 1/\beta$ ; Temperature )

**Finite temperature values** ( T = 0 → T > 0 )

$$\langle\langle\overline{\psi}_i\psi_i\rangle\rangle = \nu_i\int\frac{d^3\boldsymbol{p}}{(2\pi)^3}\frac{m_N}{\sqrt{\boldsymbol{p}^2+m_i^2}}(n_+^i - n_-^i)$$

$$\langle\langle\overline{\psi}_i\gamma^0\psi_i\rangle\rangle = \nu_i\int\frac{d^3\boldsymbol{p}}{(2\pi)^3}(n_+^i + n_-^i)$$

$$\langle\langle\overline{\psi}_i(\boldsymbol{\gamma}\cdot\mathbf{p})\psi_i\rangle\rangle = \nu_i\int\frac{d^3\boldsymbol{p}}{(2\pi)^3}\frac{\boldsymbol{p}^2}{\sqrt{\boldsymbol{p}^2+m_i^2}}(n_+^i - n_-^i)$$

- $n_\pm^i = \left[\, e^{\beta(\pm\sqrt{\boldsymbol{p}^2+m_i^2}-\mu_i^r)} + 1 \,\right]^{-1}$ ; fermion number distribution functions
- $\nu_i = 2N_fN_c$ ; degeneracy factor
  - $\nu_N = 2N_f^NN_c^N = 2\cdot2\cdot1 = 4$
  - $\nu_q = 2N_f^qN_c^q = 2\cdot2\cdot3 = 12$

$n_-^i \to n_-^i - 1$
contribution of the occupied negative energy states should be eliminated.

# Themodynamic potential density

- Thermodynamic potential density :

$$\omega_i \;=\; \langle\langle \mathcal{H}_i^{MF} \rangle\rangle - \mu_i \langle\langle \mathcal{N}_i \rangle\rangle - T \langle\langle S_i \rangle\rangle$$

where

$$\begin{aligned}\langle\langle \mathcal{H}_i^{MF} \rangle\rangle \;&=\; \langle\langle \overline{\psi}_i(\boldsymbol{\gamma}\cdot\boldsymbol{p})\psi_i \rangle\rangle - G_s^i \langle\langle \overline{\psi}_i\psi_i \rangle\rangle^2 \\ &\quad + G_v^i \langle\langle \overline{\psi}_i\gamma^0\psi_i \rangle\rangle^2 + G_{sv}^i \langle\langle \overline{\psi}_i\psi_i \rangle\rangle^2 \langle\langle \overline{\psi}_i\gamma^0\psi_i \rangle\rangle^2 \\ \langle\langle \mathcal{N}_i \rangle\rangle \;&=\; \langle\langle \overline{\psi}_i\gamma^0\psi_i \rangle\rangle \;=\; \rho_i\end{aligned}$$

$$\begin{aligned}\langle\langle S_i \rangle\rangle = -\nu_i \int \frac{d^3\boldsymbol{p}}{(2\pi)^3} \Big[\, & n_+^i \ln n_+^i + (1-n_+^i)\ln(1-n_+^i) \\ & + n_-^i \ln n_-^i + (1-n_-^i)\ln(1-n_-^i) \,\Big]\end{aligned}$$

and

$$\langle\langle \overline{\psi}_i(\boldsymbol{\gamma}\cdot\boldsymbol{p})\psi_i \rangle\rangle = \nu_i \int \frac{d^3\boldsymbol{p}}{(2\pi)^3} \frac{\boldsymbol{p}^2}{\sqrt{\boldsymbol{p}^2 + m_i^2}} (n_+^i - n_-^i)$$

Minimize $\omega_i$ w.r.t $m_i$ and $n_i^{\pm}$ $\Rightarrow$ Gap eq. and Fermion number distribution func.

# Pressure

- Pressure of nuclear and quark matters :

$$p_i(T,\mu_i) = -\left[\langle\langle \mathcal{H}_i^{MF} \rangle\rangle_{(T,\mu_i)} - \langle\langle \mathcal{H}_i^{MF} \rangle\rangle_{(T=0,\ \mu_i=m_i(T=0))}\right] + \mu_i \langle\langle \mathcal{N}_i \rangle\rangle + T \langle\langle S_i \rangle\rangle$$

where

$$\langle\langle \mathcal{H}_i^{MF} \rangle\rangle_{(T=0,\ \mu_i=m_i(T=0))} = \langle \overline{\psi}_i (\boldsymbol{\gamma}\cdot\boldsymbol{p}) \psi_i \rangle - G_s \langle \overline{\psi}_i \psi_i \rangle^2$$

$\langle \cdots \rangle$ : Zero-temperature expectation value

$$n_+^i(T=0) = \theta(\mu_i^r - \sqrt{\boldsymbol{p}^2 + m_i^2})$$

Heaviside step function

$$= \begin{cases} 1 & (\boldsymbol{p} < \sqrt{\mu_i^{r\,2} - m_i^2} \equiv \boldsymbol{p}_F^i) \\ 0 & (\boldsymbol{p} > \sqrt{\mu_i^{r\,2} - m_i^2} \equiv \boldsymbol{p}_F^i) \end{cases}$$

$\boldsymbol{p}_F^i$ : Fermi momentum

$$n_-^i(T=0) = 1$$

# Numerical Results

with $G_{sv}^{q} = 0$

# Numerical Results with $G_{sv}^{q} = 0$

- ▶ Dynamical quark mass $m_q$ vs Quark chemical potential $\mu_q$
- ▷ Quark number density $\rho_q$ vs Quark chemical potential $\mu_q$

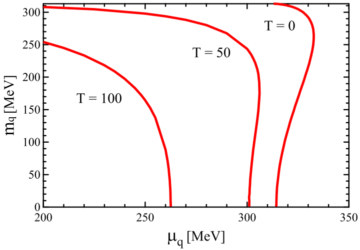


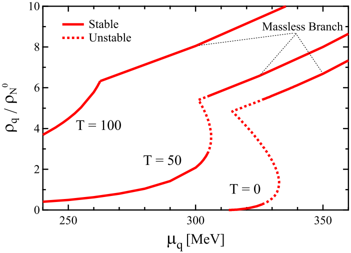


▷ Unphysical regions which have unstable solutions

Comparison of pressure

$\Rightarrow$ Determine the physically realized solution (stable solution)

▷ The solution with largest pressure = The physically realized solution

# Numerical Results with $G_{sv}^q = 0$

▶ Pressure of quark matter $p_q$
vs Quark chemical potential $\mu_q$

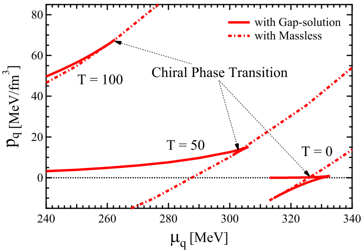


▷ Quark number density $\rho_q$
vs Quark chemical potential $\mu_q$

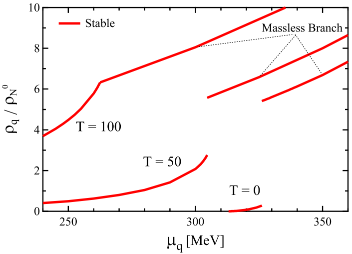


▷ $T = 0$ MeV

- $\mu_q^{\text{chiral}} \approx 326$ MeV : Chiral phase transition
- $\rho_q^{\text{coex}} = 0.28\rho_N^0 \sim 5.41\rho_N^0$ : $1^{\text{st}}$-order phase transition
  $(\rho_B = 0.09\rho_N^0 \sim 1.80\rho_N^0)$

# Numerical Results with $G_{sv}^q = 0$

▶ Pressure of quark matter $p_q$ vs Quark chemical potential $\mu_q$

▷ Quark number density $\rho_q$ vs Quark chemical potential $\mu_q$

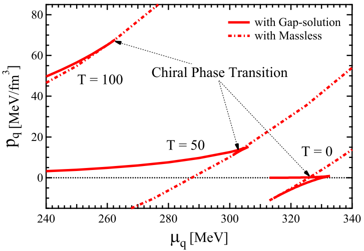


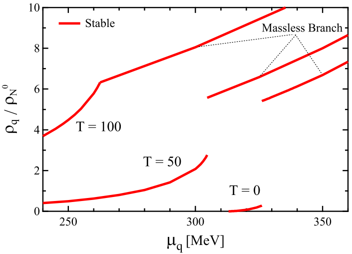


▷ $T = 50$ MeV

- $\mu_q^{\text{chiral}} \approx 305$ MeV : Chiral phase transition
- $\rho_q^{\text{coex}} = 2.76\rho_N^0 \sim 5.57\rho_N^0$ : 1st-order phase transition

  $(\rho_B = 0.92\rho_N^0 \sim 1.86\rho_N^0)$

# Numerical Results with $G_{sv}^q = 0$

▶ Pressure of quark matter $p_q$ vs Quark chemical potential $\mu_q$

▷ Quark number density $\rho_q$ vs Quark chemical potential $\mu_q$

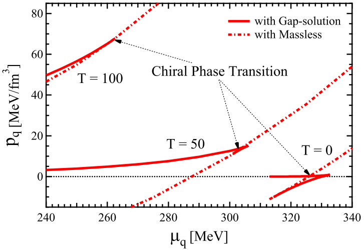


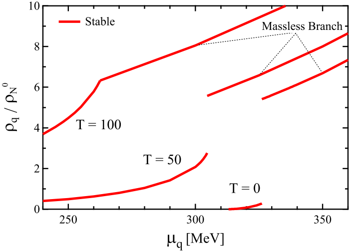


▷ $T = 100$ MeV

- $\mu_q^{\text{chiral}} \approx 263$ MeV : Chiral phase transition
- $\rho_q^{\text{chiral}} \sim 6.33\rho_N^0$ : 2nd-order phase transition*) $(\rho_B \sim 2.11\rho_N^0)$

# Numerical Results

with $G_{sv}^{q}\Lambda_{q}^{8} = -81.9$

# Numerical Results with $G^{q}_{sv}\Lambda^{8}_{q} = -81.9$

▶ Dynamical quark mass $m_q$
vs Quark chemical potential $\mu_q$

▷ Quark number density $\rho_q$
vs Quark chemical potential $\mu_q$

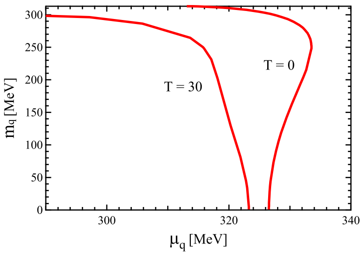


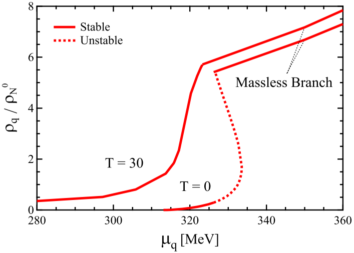


▷ Unphysical regions which have unstable solutions

Comparison of pressure

$\Rightarrow$ Determine the physically realized solution (stable solution)

▷ The solution with largest pressure = The physically realized solution

# Numerical Results with $G^q_{sv}\Lambda^8_q = -81.9$

▶ Pressure of quark matter $p_q$ vs Quark chemical potential $\mu_q$

▷ Quark number density $\rho_q$ vs Quark chemical potential $\mu_q$

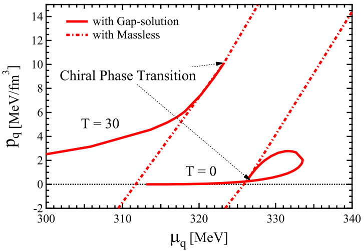


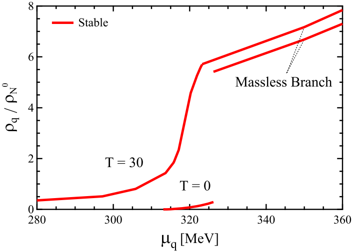


▷ $T = 0$ MeV

- $\mu_q^{\text{chiral}} \approx 326$ MeV : Chiral phase transition
- $\rho_q^{\text{coex}} = 0.29\rho_N^0 \sim 5.43\rho_N^0$ : 1st-order phase transition

  $(\rho_B = 0.10\rho_N^0 \sim 1.81\rho_N^0)$

# Numerical Results with $G^q_{sv}\Lambda^8_q = -81.9$

▶ Pressure of quark matter $p_q$ vs Quark chemical potential $\mu_q$

▷ Quark number density $\rho_q$ vs Quark chemical potential $\mu_q$

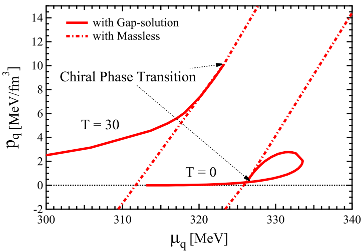


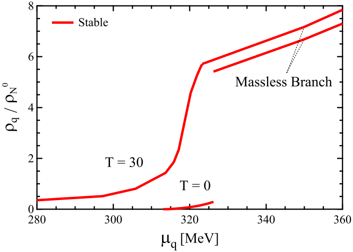


▷ $T = 30$ MeV

- $\mu_q^{\text{chiral}} \approx 323$ MeV : Chiral phase transition
- $\rho_q^{\text{chiral}} \sim 5.71\rho_N^0$ : 2nd-order phase transition*)
  $(\rho_B \sim 1.90\rho_N^0)$